

SENSORS FOR MONITORING COMPONENTS, SYSTEMS AND PROCESSES

T.Jayakumar, C.Babu Rao, John Philip, C.K.Mukhopadhyay, J.Jayapandian and C.Pandian

Indira Gandhi Centre for Atomic Research (IGCAR), Kalpakkam – 603102, India

Email: tjk@igcar.gov.in

Abstract: The application of sensors encompasses many sectors of industry. In this paper, we outline different sensors – Raman distributed temperature sensor, sensor based on nano ferrofluids and MEMS based ultrasonic sensors. The development and application of these sensors for monitoring performance of systems and processes are discussed. Further, we also discuss the application of acoustic emission and infrared thermal imaging for process monitoring.

Index terms: Fiber optic sensor, nano ferrofluids, MEMS, ultrasonic sensor. Acoustic emission, thermal imaging.

1. INTRODUCTION

The ever increasing demands on non destructive testing and evaluation has enabled the advent of new technology and sensors. In this paper, we describe the development and application of a few of these sensors namely Raman distributed temperature sensor, microelectro mechanical ultrasonic sensor, nano ferrofluids based sensors, acoustic emission sensors and infrared sensors.

2. RAMAN DISTRIBUTED TEMPERATURE SENSOR

Raman distributed temperature sensor (RDTS) was first demonstrated in 1985 by Dakin and Pratt [1]. RDTS is used in varied industries for different applications like oil pipeline monitoring [2], power cable monitoring [3],

geothermal temperature monitoring and so on.

A programme on development of RDTS for deployment on sodium circuits in Fast Breeder Reactors (FBR) was undertaken at IGCAR in collaboration with Raja Ramanna Centre for Advanced Technology(RRCAT), Indore. The objective of the programme is distributed temperature measurement along the sodium circuits.

2.1 PRINCIPLE

In the RDTS system, a laser pulse is launched into an optical fiber. The backscattered Stokes and anti-Stokes lines of the laser are separated and their intensities measured. The ratio of the intensity of the anti-Stokes to that of Stokes line is a measure of the temperature [4-6].

$$\frac{I_A}{I_S} = \frac{(\nu_0 + \nu_r)^4}{(\nu_0 - \nu_r)^4} \exp\left(\frac{-hc\nu_r}{kT}\right)$$

From the time of flight of the laser pulse, the scattering point/temperature measurement zone can be located. The temperature measured is an integral value over one pulse width of the laser. This defines the two point spatial resolution of the RDTS [7, 8].

$$\text{Spatial Resolution} = w * \frac{c}{n_g}$$

Where w is the pulse width, c is the velocity of light and n_g is the refractive index of the material of the fiber.

2.2 TEST LOOP

In order to assess the feasibility of this technique for sodium circuits of FBR, RDTS is first deployed on a test loop and detailed studies were conducted under simulated conditions.

The loop structure is made of SS 304 pipes of 100NB diameter. This pipe structure is similar to sodium loops in Fast Breeder Reactors. The length of the entire loop is 30.5 m. The loop consists of six linear sectors and five

bends as shown in Fig. 1.



Fig. 1. Test loop to test optical fiber based distributed sensor for temperature sensor

To evaluate the performance of the distributed temperature measurement of RDTS, provision is made to heat the loop to maintain any chosen temperature profile. Conventional temperature sensor, K-Type (Chromel-Alumel) thermocouple, which is widely used in reactor applications, is used to evaluate the performance of the RDTS system.

2.3 FIBER LAYING

Since temperature in sodium circuits of FBR exceeds 550°C (973K), conventional aluminium coated or copper coated high temperature fiber cannot be employed due to the oxidation of the coating at elevated temperature. Therefore, gold coated fiber ($50\mu\text{m}/125\mu\text{m}$) is chosen as sensor fiber. Also our experience had shown that the bare fibers mounted on the sodium loop are prone to damage due to mechanical/ thermal stresses. Therefore the sensor fiber is encased in SS capillary of 2mm internal diameter. The SS capillary is laid on the SS pipe, in direct contact, through spot welding, for maximum transference of heat from SS pipe to SS capillary containing fiber. The fiber laid on the loop, thus, is covered with insulating material – glass wool. The entire set up is then encapsulated by aluminium metal clad. The glass wool and the metal clad prevent heat leakage from the loop to the surroundings.

2.4 TEMPERATURE MEASUREMENT

The RDTS with gold coated fiber is able to monitor temperature up to 700°C with a spatial resolution of 1m

and temperature resolution of 5°C (Fig. 2). Since the RDTS represents two readings, from bottom to top and top to bottom of a loop as explained above, the temperature reading shown in Fig. 2 is symmetrical around 78.8m. The temperature measurement on the left of 78.8 meter is a mirror reflection of the temperature measurement on to its right. The small drop in temperature measurement seen on the right can be attributed to attenuation. The minor variations are due to macro bends / micro bends accrued on fiber while fiber laying which are not symmetrical.

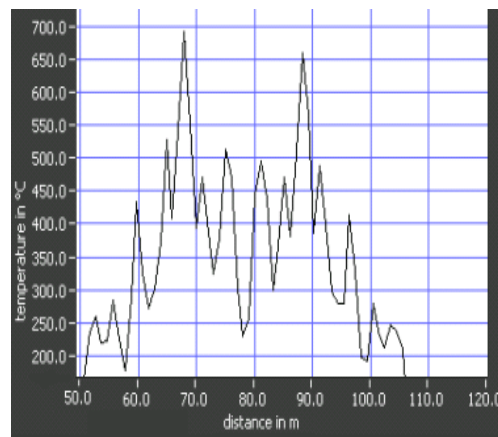


Fig. 2. Temperature measurement on the loop using RDTS

3. CAPACITIVE MICRO ELECTROMECHANICAL ULTRASONIC TRANSDUCER (cMUT)

MEMS based capacitive Micromachined Ultrasonic Transducer (cMUT) is a next generation ultrasonic sensor which has several advantages like higher bandwidth, non-contact, etc. over conventional piezoelectric transducers [9]. These transducers find potential applications in non destructive testing and medical imaging. At IGCAR, cMUT sensors for non destructive evaluation of main vessel and safely vessel of the prototype fast breeder reactor (PFBR) are designed and fabricated in collaboration with IISc, Bangalore and CEERI, Pilani. The resonance frequency of these sensors is evaluated using Laser Doppler Vibratometer and is found to be 2.4 MHz which is as per the simulated results. Fabricated cMUTs are further characterized for their functionality and the feedback is used for optimisation of the design and fabrication procedure for the cMUTs.

3.2 cMUT FABRICATION & CHARACTERIZATION

3.2.1. cMUT FABRICATION

cMUT is similar to condenser microphone i.e. electrostatic method of generating / receiving ultrasonic waves. Although this method of generating ultrasonic waves is well known for years, was not popular due to the requirement of high electric fields that need to be maintained between electrodes to achieve acceptable efficiencies. Only with the advent of micro-fabrication technology which made it possible to achieve the submicron gaps between electrodes thus permitting higher fields between them. Complete details about the design and fabrication of cMUT devices are given elsewhere [10]. Dimensions of the fabricated single cell are shown in Fig. 3 and the packaged device consisting of 5X5 and 1X5 cMUT arrays is shown in Fig. 4.

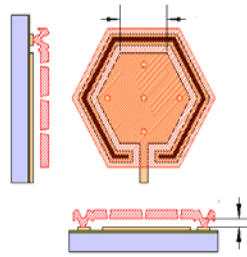


Fig. 3. cMUT single cell

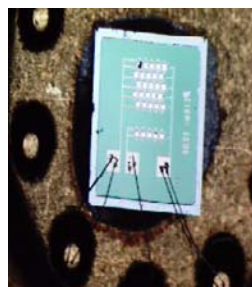


Fig. 4. . Packaged cMUT 5X5 and 5X1 array

3.2.2. cMUT CHARACTERIZATION

Capacitances of the 5X1 and 5X5 arrays were measured using Quadtech precision LCR meter (Model No:1920) and it was found that the elements of the array were showing variations in the capacitance value against an expected value in the order of a few pF. Apart from this, these sensors showed unexpected low resistive value and could not be electrically characterized [11]. Dektak stylus profiler was used to study the surface profile of cMUT array and membrane deformation during the application of a dc voltage. Figure 5 shows the profile of a single cell of cMUT without and with an applied dc field of 9V. Although the expected height of membrane (1 μm) from the substrate is seen in this figure, the surface roughness of the electrode coating is large ($\approx 1 \mu\text{m}$) and it is also clear from this figure that there is no deformation taking place in the membrane due to the applied dc voltage.

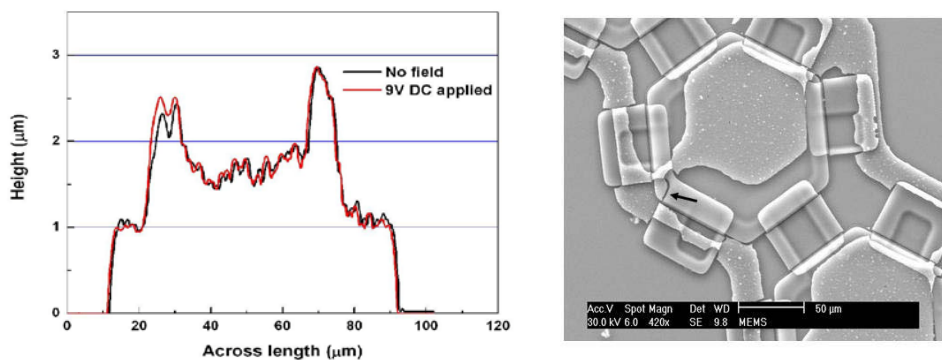


Fig. 5. Surface Profile Single cMUT Array. with and without field.

Fig. 6. SEM Image of a of a Single cMUT cell

SEM studies were undertaken on these devices using Phillips scanning electron microscopy (model no: ESEM XL-30). Figure 6 shows the SEM image of one of the cMUT cells of 5X1 array. From this figure, it is clear that the Al electrode coating is not centered on the membrane and is not uniform. Similarly, a micro crack was observed on the left side of all the cells (shown by an arrow).

Apart from this, resonance study was also undertaken with network analyzer [11]. From all these studies, it is concluded that the improper coating of Al electrode, could be the reason for the non-functionality of the devices. This feedback helped towards successful fabrication of next round of cMUT arrays and devices.

4. NANO FERRO FLUIDS

Ferrofluid is a stable suspension of nanometer sized magnetic particles in an aqueous or organic carrier fluid. It is a unique material that has both the liquid and magnetic properties. Such fluids have been found to have several fascinating applications such as flux leakage measurement sensors, magneto-optical wavelength filter, optical modulators, nonlinear optical materials, tunable optical filters, optical gratings and optical switches.

4.1 NANOFLUID BASED FLUX LEAKAGE SENSOR

By taking advantage of the ordering property of the ferrofluid, we have invented a new application for this fluid to detect defects in ferromagnetic materials and components based on magnetic flux leakage (MFL) technique. To realize this, we have developed highly monodispersed magnetic emulsions with droplets in the size range of 150 to 300 nanometers. These emulsions are very easy to manipulate by an external magnetic field. Changing of color can be seen in such an oriented ferrofluid, due to Bragg phenomenon (due to one-dimensional ordering of colloidal droplets).

Use of ferrofluid based emulsions enables quantification of discontinuities in materials with high reliability [12]. Here, depending upon the strength of the leakage magnetic field, the ferrofluid emulsion switches its color from one to another in the visible spectra (VIBGYOR). For example, when the magnetic field changes from a higher to a lower value, the color of the fluid changes from violet to green or yellow or orange or red, depending upon the magnitude of the leakage magnetic field.

A photograph of the colour pattern observed in the ferrofluid cell due to the normal component of the leakage magnetic field in the absence (left) and presence of a rectangular slot (right) is shown in Fig. 7.

For the rectangular slot, the leakage magnetic field value is the maximum at 2.0 mm away on both sides of

the slot centre. At the centre of the slot ($x=0$), the leakage field strength is zero, whereas the tangential component of the leakage field is maximum at the centre. Therefore, at the centre of the discontinuity, the expected leakage field is zero and therefore the droplets in the ferrofluid cell remain in their random orientation. As a result, the color in the region will be the natural colour of the emulsion. On both sides of the crack centre, the variation in the field is symmetrical but in opposite directions.

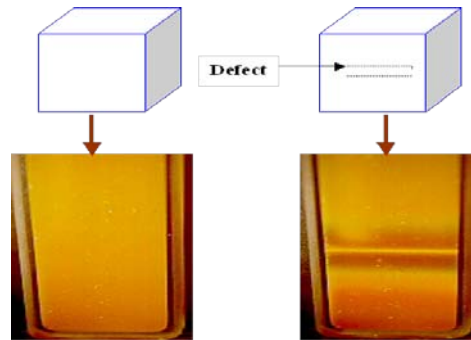


Fig. 7. A photograph of the colour pattern observed in the ferrofluid cell.

4.2 TUNABLE OPTICAL FILTER

In order to overcome the problems associated with conventional bandpass filters, a tunable type of optical filter has been developed at IGCAR [13]. The filter comprises of ferrofluid-based emulsion cell, a miniature solenoid and a variable direct current source for changing the magnetic field. By varying the magnetic field, the filter can be tuned to select the desired wavelength. Figure 8 shows the variation in the intensity of the Bragg reflected wavelength, at different magnetic fields.

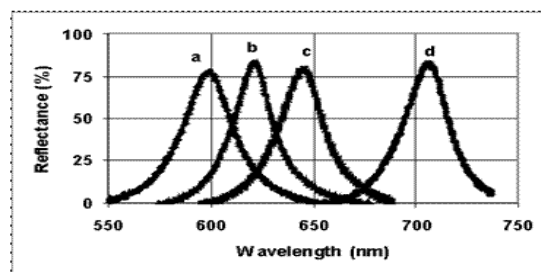


Fig. 8. Variation in intensity of Bragg reflected light with wavelength at different magnetic fields (The field strength values are a= 258 Gauss; b = 194 Gauss; c = 140 Gauss; d = 98 Gauss).

The main advantages of this new optical filter are (a) a single filter can be used for a range of central wavelengths, where the desired central wavelength region can be tuned by external magnetic field, (b) it is suitable for selecting wavelengths in the ultraviolet, visible and infrared regions, (c) there is no need for changing the optical element for different wavelength regions, (d) tuning can be easily achieved by changing the field strength, (e) the spectral distribution can be controlled by adjusting the polydispersity of the emulsion, (f) the intensity of the transmitted light can be controlled by changing the emulsion concentration, and (g) it is simple to operate and less expensive compared to the existing filters.

5. ON-LINE MONITORING OF WELDING PROCESSES USING NDE TECHNIQUES

Acoustic emission technique (AET) is utilised for detection and location of dynamic defects (i.e. as and when they form or grow), as a welding process progresses. The generation of elastic waves due to strain energy released during the formation of defects and consequent detection of these elastic waves using piezoelectric based transducers is the main basis of AET for monitoring of welding processes. The defects that can be detected, located and qualitatively evaluated by AET are (i) nucleation and growths of cracks during welding and cooling (delayed cracking), (ii) slag inclusions, (iii) micro fissuring, (iv) cold and hot cracking, (v) reheat cracks and (vi) weld cracking associated with phase transformations. Once these defects are detected and located by AET, other NDT methods can be used for detailed analysis, if needed. AET has been successfully used for on-line monitoring of welds prepared by TIG, submerged arc, electro slag welding, etc. However, non-slag forming welding processes are particularly suitable for AE monitoring. The main problem in AE monitoring of welding process is the elimination of unwanted signals due to slag cracking and electromagnetic influence from the arc. Various methodologies are used to eliminate noise by proper signal conditioning and advanced digital signal processing techniques.

Thermal imaging or infrared imaging is an advanced, non destructive evaluation method based on the detection

of infrared radiations emitted by the object. It makes use of the infrared band of the electromagnetic spectrum. Infrared refers to a region of the electromagnetic spectrum between the visible and microwave. The IR spectrum extends from 0.75 μm to 1000 μm . The properties of infrared radiations are similar to other electromagnetic radiations such as light. They travel in straight lines; propagate in vacuum as well as in liquids, solids and gases. They can be optically focused and directed by mirrors and lenses. The laws of geometrical optics are valid for these also. The energy and intensity of infrared radiation emitted by an object primarily depends on its temperature and can be calculated using the analytical tools such as Wein's law, Planck's law and Stefan Boltzmann law.

5.1 EVALUATION OF RESISTANCE SPOT WELDS BY ACOUSTIC EMISSION AND THERMOGRAPHY TECHNIQUES

Acoustic emission and thermography techniques were used for on-line monitoring of resistant spot welding process [15-17]. A number of carbon steel sheets of approximately 1.6 mm thickness were spot welded by making use of 45-kVA capacity portable spot welding machine. Spot welding trials were carried out at different welding conditions (representing struck weld, good weld and splash weld conditions) by adjusting the phase shift setting and the weld time. Figure 9 shows the variation of RMS voltage of the AE signal with time for good weld and bad weld. Bad quality welds are observed to generate reduced AE activity in comparison to good welds.

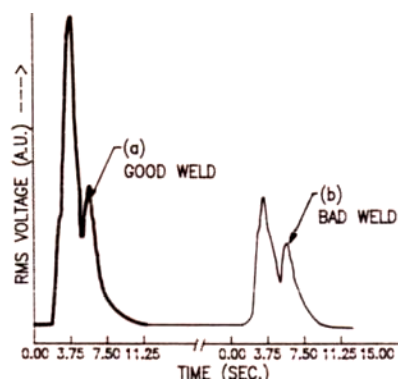


Fig. 9. Variation in AE RMS voltage with time for (a) good weld and (b) bad weld

Figure 10 shows the thermal images of a good weld and that of a weld made with reduced current. Analysis of a number of welds indicated that the heat distribution in a good weld is uniform and symmetric about the centre of the weld (fig 10a), whereas bad welds have irregular thermal patterns (fig 10b).

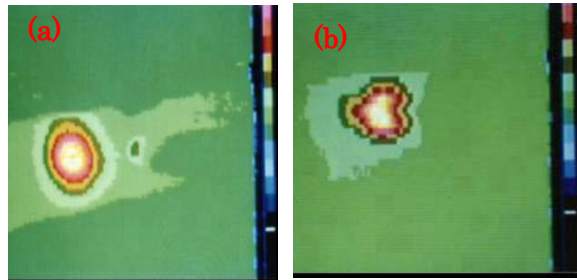


Fig. 10. Thermograms of (a) good weld and (b) of bad weld

5.3 MONITORING OF END CAP WELDING OF NUCLEAR FUEL ELEMENTS

End cap welding is used in the assembly of nuclear fuel elements. The AE signals generated during the welding stage as well as during the post-weld stage were found useful to discriminate normal welds from welds with presence of defects [14-16]. Higher acoustic activity was generated for tubes welded with presence of various defects as compared to the AE generated during welding of tubes without any defects i.e. normal weld (Fig. 11).

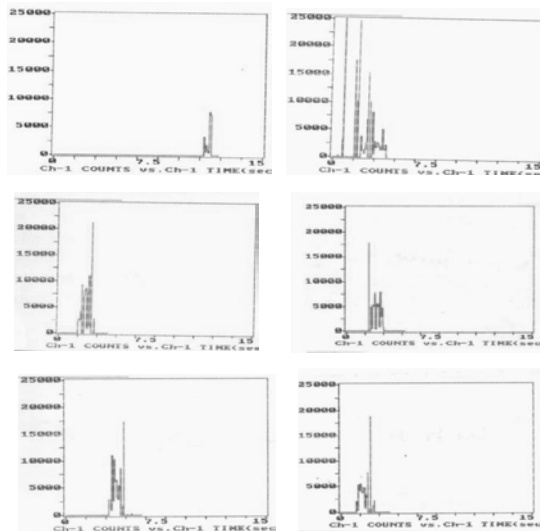


Fig. 11. AE Counts observed during end cap welding with defects generated by variation in weld parameters

It has been observed that two separate clusters (normal welds and welds with presence of defects) are formed corresponding to the two weld categories. Thermal imaging carried out on these elements after the welding process indicated that it is possible to detect most of the imperfections very confidently [14-16]. In general, good welds are characterised by uniform isothermal widths and symmetrical isothermal patterns (Fig. 12(a)) while bad welds are characterised by uneven isothermal widths and patterns (Fig. 12(b)). By thermography, the circumferential location where the defect had occurred could also be indicated.

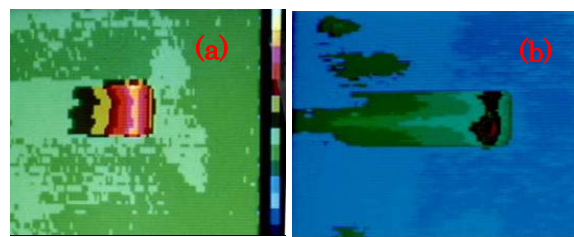


Fig. 12. Thermal images of (a) a normal weld and (b) a weld with excess graphite coating

ACKNOWLEDGEMENTS

The authors are thankful to Dr. Baldev Raj, Director, IGCAR, for constant encouragement and support. The authors are also thankful to Dr.Sanjay Kher, RRCAT, Indore, for his contribution in development of RDTS.

REFERENCES

- [1]. Dakin, Pratt, Distributed Optical Fibre Raman Temperature Sensor Using A Semiconductor Light Source And Detector, *Electronics Letters* 20th June 1985 Vol. 21 No. 13
- [2]. M. Niklès, B. Vogel, F. Briffod, S. Grosswig, F. Sauser, S. Luebbecke, A. Bals, T. Pfeiffer, "Leakage detection using fiber optics distributed temperature monitoring", *Smart Struct. and Mat.* 2004: Smart Sensor Techn. and Meas

- [3]. GunesYilmaz, A distributed optical fiber sensor for temperature detection in power cables *Sensors and Actuators A*, Vol125, pg148-155,2006
- [4]. Gabriele Bolognini et al, Analysis of distributed temperature sensing based on Raman scattering using OTDR coding and discrete Raman amplification, *Meas. Sci. Technol.* 18 (2007) 3211–3218
- [5]. O.lida et al, Expansion of Measuring Range for a Fiber-optic Distributed Temperature sensor and Applications to Commercial Plants, IMTC '94 May 10-12, Hamamatsu, 1994
- [6]. Mostafa Ahangrani Farahani and Torsten Gogolla , Spontaneous Raman Scattering in Optical Fibers with Modulated Probe Light for Distributed Temperature Raman Remote Sensing, *Journal Of Lightwave Technology*, Vol. 17, No. 8, August 1999 ,
- [7]. Boiarski et al, Temperature Measurements in Power Plant Equipment Using Distributed Fiber Optic Sensing, *IEEE Transactions on Power Delivery*, Vol. 10, No. 4. October 1995
- [8]. Gunes Yilmaz, A distributed optical fiber sensor for temperature detection in power cables *Sensors and Actuators A*, Vol125, pg148-155,2006
- [9]. I. Ladabaum, et.al. *IEEE Trans. Ultrason., Ferroelect., Freq. Contr.*, vol. 45, pp. 678–690, May 1998.
- [10]. A. Arora, et.al., *Sensors & Transducers Journal*, Vol. 93, Issue 6, June 2008, pp. 15-20.
- [11]. J. Jayapandian, et.al, "Report on the recent batch of fabricated cMUT Devices", IGCAR Internal report, 2008.
- [12]. J.Philip, C.Babu Rao, T.Jayakumar & B.Raj, *NDT&E International*, 33 (2000) 289-295; Patent No. 186620
- [13]. J.Philip, T.Jayakumar, P.Kalyanasundaram , B.Raj, *Meas. Sci. & Tech.*. 14 (2003) 1289-1294; Patent No. 196063.
- [14]. Baldev Raj, B.Venkatraman, T.P.S.Gill and T.Jayakumar, Reliable Quality through Intelligent Welding Methodologies, *Proc. Int Conf. IMACS-IEEE99*, Athens, Greece, June 1999.
- [15]. Baldev Raj, B.Venkatraman, C.K.Mukho-padhyay, T.Jayakumar, A.Lakshminarayana, N.Saratchandran and Ashok Kumar, Intelligent Welding using NDE Sensors, *Proc. European Conference on NDT*, Copenhagen, May, 1998, pp. 1244-1250.

- [16]. Baldev Raj, T.Jayakumar and B.Venkatraman, Intelligent Welding, Proc. Int. Conf. Recent Advances in Metallurgical Processes, IISc, Bangalore, eds. D.H.Sastry, E.S.Dwarakadasa, G.N.K.Iyengar and S.Subramanian, New Age International Publ., New Delhi, Vol.2, 1997, pp. 1035-1046.